



# Marine and freshwater micropearls: biomineralization producing strontium-rich amorphous calcium carbonate inclusions is widespread in the genus *Tetraselmis* (Chlorophyta)

Agathe Martignier<sup>1</sup>, Montserrat Filella<sup>2</sup>, Kilian Pollok<sup>3</sup>, Michael Melkonian<sup>4</sup>, Michael Bensimon<sup>5</sup>, François Barja<sup>6</sup>, Falko Langenhorst<sup>3</sup>, Jean-Michel Jaquet<sup>1</sup>, and Daniel Ariztegui<sup>1</sup>

<sup>1</sup>Department of Earth Sciences, University of Geneva, Geneva, 1205, Switzerland

<sup>2</sup>Department F.-A. Forel, University of Geneva, Geneva, 1205, Switzerland

<sup>3</sup>Institute of Geosciences, Friedrich Schiller University Jena, Jena, 07745, Germany

<sup>4</sup>Botany Department, Cologne Biocenter, University of Cologne, Cologne, 50674, Germany

<sup>5</sup>EPFL ENAC IIE GR-CEL IsoTraceLab, EPFL, Lausanne, 1015 Switzerland

<sup>6</sup>Microbiology Unit, University of Geneva, Geneva, 1205, Switzerland

**Correspondence:** Agathe Martignier (agathe.martignier@unige.ch)

Received: 23 April 2018 – Discussion started: 2 May 2018

Revised: 5 September 2018 – Accepted: 16 October 2018 – Published: 7 November 2018

**Abstract.** Unicellular algae play important roles in the biogeochemical cycles of numerous elements, particularly through the biomineralization capacity of certain species (e.g., coccolithophores greatly contributing to the “organic carbon pump” of the oceans), and unidentified actors of these cycles are still being discovered. This is the case of the unicellular alga *Tetraselmis cordiformis* (Chlorophyta) that was recently discovered to form intracellular mineral inclusions, called micropearls, which had been previously overlooked. These intracellular inclusions of hydrated amorphous calcium carbonates (ACCs) were first described in Lake Geneva (Switzerland) and are the result of a novel biomineralization process. The genus *Tetraselmis* includes more than 30 species that have been widely studied since the description of the type species in 1878.

The present study shows that many other *Tetraselmis* species share this biomineralization capacity: 10 species out of the 12 tested contained micropearls, including *T. chui*, *T. convolutae*, *T. levis*, *T. subcordiformis*, *T. suecica* and *T. tetrahele*. Our results indicate that micropearls are not randomly distributed inside the *Tetraselmis* cells but are located preferentially under the plasma membrane and seem to form a definite pattern, which differs among species. In *Tetraselmis* cells, the biomineralization process seems to systematically start with a rod-shaped nucleus and results in an enrichment of the micropearls in Sr over Ca (the Sr/Ca ra-

tio is more than 200 times higher in the micropearls than in the surrounding water or growth medium). This concentrating capacity varies among species and may be of interest for possible bioremediation techniques regarding radioactive <sup>90</sup>Sr water pollution.

The *Tetraselmis* species forming micropearls live in various habitats, indicating that this novel biomineralization process takes place in different environments (marine, brackish and freshwater) and is therefore a widespread phenomenon.

## 1 Introduction

The biogeochemical cycles of numerous elements are influenced by the biomineralization capacities of certain unicellular organisms. This is the case, for example, of the coccolithophores, which play an important role in the carbon cycle through their production of biogenic calcite (Bolton et al., 2016). Amorphous calcium carbonate (ACC) is also an important actor in the biogenic carbonate cycle because it is a frequent precursor of calcite, as many organisms use ACC to build biominerals with superior properties (Albéric et al., 2018; Rodriguez-Blanco et al., 2017). For example, the precipitation of calcium carbonate in microbial mats, the Earth's earliest ecosystem, starts with an amorphous calcite

gel (Dupraz et al., 2009), and the formation of ACC inside tissue could make coral skeletons less susceptible to ocean acidification (Mass et al., 2017).

In unicellular organisms, intracellular inclusions of ACC had, at first, only been described in cyanobacteria (Couradeau et al., 2012; Benzerara et al., 2014; Blondeau et al., 2018). More recently, similar inclusions have been described in unicellular eukaryotes of Lake Geneva (Switzerland). Consisting of hydrated ACCs but frequently enriched in alkaline-earth elements (e.g., Sr or Ba) and typically displaying internal oscillatory zonation, these inclusions have been named micropearls (Jaquet et al., 2013; Martignier et al., 2017). The internal zonation is due to variations in the Ba/Ca or Sr/Ca ratios.

Until now, micropearls had been observed only in two freshwater species: the unicellular green alga *Tetraselmis cordiformis* (Chlorodendrophyceae, Chlorophyta) producing micropearls enriched in Sr and a second freshwater microorganism producing micropearls enriched in Ba, yet to be identified (Martignier et al., 2017). Since its first description in 1878 (Stein, 1878), the genus *Tetraselmis* has been much studied by biologists because several species are economically important due to their high nutritional value and ease of culture (Hemaiswarya et al., 2011). *Tetraselmis* species are used extensively as aquaculture feed (Azma et al., 2011; Lu et al., 2017; Park and Hur, 2000; Zittelli et al., 2006) and some have been suggested as potential producers of biofuels (Asinari di San Marzano et al., 1981; Grierson et al., 2012; Lim et al., 2012; Montero et al., 2011; Wei et al., 2015). They have also served as models in algal research (Douglas, 1983; Gooday, 1970; Kirst, 1977; Marin et al., 1993; Melkonian, 1979; Norris et al., 1980; Regan, 1988; Salisbury et al., 1984).

The motile cells of *Tetraselmis* have four scale-covered flagella, which emerge from an anterior (or apical) depression of the cell (Manton and Parke, 1965). The *Tetraselmis* genus has a cell wall formation process that is unique among green algae as the cells synthesize small non-mineralized scales in the Golgi apparatus, which undergo exocytosis through Golgi-derived secretory vesicles to form a solid wall (theca) composed of fused scales (Becker et al., 1994; Domozych, 1984; Manton and Parke, 1965). Regarding their habitat, most *Tetraselmis* species are free-living (planktonic or benthic) (Norris et al., 1980), although some species live in specialized habitats, for example as endosymbiont in flatworms (Parke and Manton, 1967; Trench, 1979; Venn et al., 2008). *Tetraselmis cordiformis* is presumably the only freshwater species among the 33 species currently accepted taxonomically in the genus *Tetraselmis* (Guiry and Guiry, 2018).

However, mineral inclusions had never been described in these microorganisms until the recent observation of micropearls in *Tetraselmis cordiformis* (Martignier et al., 2017). The fact that this new physiological trait had gone unnoticed is puzzling, especially as *Tetraselmis cordiformis* is the type species of the genus. This can probably be explained by the

translucence of the micropearls under the optical microscope and their great sensitivity to pH variations, leading to their alteration or dissolution during most sample preparation techniques (Martignier et al., 2017).

Interestingly, several *Tetraselmis* species (e.g., *T. subcordiformis*) have been mentioned as potential candidates for radioactive Sr bioremediation due to their high Sr absorption capacities (Fukuda et al., 2014; Li et al., 2006), but the precise process by which these microorganisms concentrate this element has never been determined.

The present study investigates 12 species of the genus *Tetraselmis*, including the freshwater *Tetraselmis cordiformis*, with the objective of understanding whether the biomineralization process leading to the formation of micropearls is common to the whole genus or is restricted to *T. cordiformis*. Species living in contrasting environments have been selected to also evaluate if the formation of micropearls is linked to their habitat. Each species is represented by one or several strains, obtained from public algal culture collections. All analyses were carried out on cells sampled from these cultures on the day of their arrival in our laboratory. The micropearls were imaged by scanning electron microscopy (SEM), and their composition was measured by energy-dispersive X-ray spectroscopy (EDXS). The inner structure and chemical composition of micropearls in three different species were studied by transmission electron microscopy (TEM) on focused ion beam (FIB) cross sections.

## 2 Samples and methods

### 2.1 Origin of the samples and pre-treatment methods

Culture samples of 12 different *Tetraselmis* species were obtained from three different algal culture collections and were grown in different media (Table 1). The recipe of each growth medium is available on the website of the respective culture collections (Table S1 in the Supplement). A single strain of each species was studied, except for *T. chui* (two strains) and *T. cordiformis* (three strains). Table 1 lists the strain names. Most cells in these cultures were mature at the time of observation for this study.

Samples for microscopic observation of each strain were prepared directly after the organisms' arrival in our laboratory: small portions of the culture (without any change of the original medium) were filtered under moderate vacuum (−20 to −30 kPa) on polycarbonate filter membranes with 0.2, 1 or 2 µm pore sizes. Volumes filtered (variable depending on culture concentration) were recorded. Species issued from SAG (Sammlung von Algenkulturen – University of Göttingen, Germany) were grown on agar and, therefore, cultures had to be resuspended just before filtration. Filter membranes were dried in the dark at room temperature after filtration. A total of 458 micropearls were analyzed by EDXS.

**Table 1.** Specific information for each species and their culture conditions. Providers include the following. CCAC: Culture Collection of Algae at the University of Cologne (Germany) – <http://www.ccac.uni-koeln.de/>, last access: 6 July 2018; SAG: Sammlung von Algenkulturen at the University of Göttingen (Germany) – <https://www.uni-goettingen.de/de/184982.html>, last access: 6 July 2018; AC: Algobank – culture collection of microalgae of the University of Caen (France) – <https://www.unicaen.fr/algobank/accueil/>, last access: 6 July 2018; TCC: Thonon Culture Collection of the CARTEL of Thonon-les-Bains (France) – <https://www6.inra.fr/carrtel-collection>, last access: 6 July 2018. All culture media compositions are given on the corresponding websites (detailed addresses in Table S1).

	Origin of the sample	Approx. micropearl size	Culture medium	Provider strain no.	Abbreviation
<i>Chlamydomonas</i>					
<i>C. reinhardtii</i>	Freshwater France	no micropearls observed	L-C	TCC 778	–
<i>C. intermedia</i>	Freshwater France, Lake Geneva	no micropearls observed	L-C	TCC 113	–
<i>Tetraselmis</i>					
<i>T. ascus</i>	Marine Spain, Canary Islands, Gran Canaria	no micropearls observed	ASP-12	CCAC 3902	
<i>T. chui</i>	Marine Germany, Heligoland	0.7 µm length	ASP-H	CCAC 0014	chui_cc
	Marine Scotland, Millport, Clyde estuary	0.7 µm length	1/2 SWEg Ag	SAG 8–6	chui_sa
<i>T. contracta</i>	Marine France, Brittany, Île de Batz	1.2 µm length	ASP-H	CCAC 1405	contract_cc
<i>T. convolutae</i>	Marine (symbiotic in flatworm) France, Brittany, Île de Batz	0.8 µm length	ASP-H	CCAC 0100	convol_cc
<i>T. cordiformis</i>	Freshwater Germany, Cologne, Lake Fühlinger	1 µm diameter	SFM	CCAC 0051	cord-F_cc
	Freshwater Germany, Münster, castle ditch	1 µm diameter	Waris – H	CCAC 0579B	cord-M_cc
	Freshwater strain 0579B obtained from CCAC	1 µm diameter	Diat	SAG 26.82	cord-M_sa
<i>T. desikacharyi</i>	Marine France, Île de Batz, Rochigou	0.9 µm length	ASP-H	CCAC 0029	desika_cc
<i>T. levis</i>	Marine France, Saint-Gilles-Croix-de-Vie	0.6 µm length	ES	AC 257	levis_ac
<i>T. marina</i>	Marine strain CA5, from L. Provasoli	no micropearls observed	Porph Ag	SAG 202.8	
<i>T. striata</i>	Marine UK, North Wales, Conwy	0.6 µm length	SWES Ag	SAG 41.85	striata_sa
<i>T. subcordiformis</i>	Marine USA, Connecticut, New Haven	0.4 µm length	Porph Ag	SAG 161-1a	subcord_sa
<i>T. suecica</i>	Marine UK, Plymouth	0.7 µm length	ES	AC 254	suecica_ac
<i>T. tetrathele</i>	Marine –	0.9 µm length	ES	AC 261	tetrath_ac

## 2.2 Water chemistry measurements

Elemental composition of each culture medium was measured at the IsoTraceLab (EPFL, Lausanne, Switzerland), except for the ES medium for which we could not obtain a sample. Blank samples of Milli-Q water were bottled at the same time as growing medium samples and measured in the same way (Table S2). Barium and Sr were measured by inductively coupled plasma sector field mass spectrometry (ICP-SFMS) using a Finnigan™ Element2 high-performance high-resolution ICPMS model. The mass resolution was set to 500

to increase analytical sensitivity. Calibration standards were prepared through successive dilutions in cleaned Teflon bottles of 0.1 g L<sup>-1</sup> ICPMS stock solutions (TechLab, France). Suprapur™-grade nitric acid (65 % Merck) was used for the acidification in the preparation of standards. Ultrapure water was produced using Milli-Q™ ultrapure water system (Millipore, Bedford, USA). Rhodium was used as the internal standard for samples and standards to correct signal drift.

At this resolution mode, the sensitivity was better than 1.2 × 10<sup>6</sup> cps ppb<sup>-1</sup> of <sup>115</sup>In. The measurement repeatability expressed in terms of relative standard deviation (RSD) was

better than 5 %. The accuracy of the method was tested using a homemade standard solution containing  $5.0 \text{ ng L}^{-1}$ , used as a reference. Accuracy was better than 5 %. The detection limits obtained for Sr and Ba was around  $100 \text{ ng L}^{-1}$  under these experimental conditions. Note that for the ES medium (not analyzed), the concentrations were set as equivalent to standard sea water, i.e.,  $\text{Sr} = 9 \times 10^{-5} \text{ M}$  and  $\text{Ca} = 10^{-2} \text{ M}$ , giving a ratio of  $\text{Sr}/\text{Ca} = 9 \times 10^{-3}$ .

### 2.3 Scanning electron microscopy (SEM) and EDXS analysis

Small portions of the dried filters were mounted on aluminium stubs with double-sided conductive carbon tape and then coated with gold (ca. 10 nm) using low vacuum sputter coating. A JEOL JSM-7001F scanning electron microscope (Department of Earth Sciences, University of Geneva, Switzerland), equipped with an EDXS detector (model EX-94300S4L1Q; JEOL), was used to perform EDXS analyses and to obtain images of the dried samples. Semiquantitative results were obtained using the ZAF correction method. Samples were imaged with backscattered electrons. This method allows us to clearly locate the micropearls inside the organisms thanks to the high difference of mean atomic numbers between the micropearls and the surrounding organic matter. EDXS measurements were acquired with settings of 15 kV accelerating voltage, a beam current of  $\sim 7 \text{ nA}$  and acquisition times of 30 s. Semiquantitative EDXS analyses of elemental concentrations were made without taking carbon, nitrogen and oxygen into account. EDXS results are all presented as mol %.

### 2.4 Counts and statistics lead on the *Tetraselmis* culture cells

Counts were performed on the images obtained by SEM. The counts showed that the agar medium seems to hinder the growth of micropearls. These strains were therefore not taken into account for the statistics. Two strains of *Tetraselmis cordiformis* and two strains of *Tetraselmis chui* were analyzed. The samples of the two *Tetraselmis cordiformis* strains taken on their first day of arrival were damaged during sample preparation due to a too high filtration pressure, destroying the arrangement of the micropearls in the cells. A sample obtained from one of these strains 60 days after arrival was therefore taken into account for the statistics, in replacement.

The preservation of the pattern of micropearl arrangement in the cell is difficult during sample preparation, as it is easily disturbed. The following parameters directly influence the preservation of that feature: the fragility of the cells (*T. contracta* cells, for example, seem very solid while *T. chui* cells seem more fragile) and sample preparation methods (e.g., pressure during filtration; see difference between e and f in Fig. S1 in the Supplement).

## 2.5 Focused ion beam (FIB) preparation

Electron-transparent lamellae for TEM were prepared with a FIB–SEM workstation (FEI Quanta 3D FEG at the Institute of Geosciences, Friedrich Schiller University Jena, Germany). The cells were previously selected based on SEM imaging. To protect the sample, a platinum strap of 15 to  $30 \mu\text{m}$  in length,  $\sim 3 \mu\text{m}$  wide and  $\sim 3 \mu\text{m}$  high was deposited on the cell during lamella preparation, via ion-beam-induced deposition using the gas injection system (GIS). Stepped trenches were prepared on both sides of the Pt straps by Ga+ ion beam sputtering. This operation was performed at 30 keV energy and a 3 to 5 nA beam current.

The resulting lamellae were then thinned to approximately  $1 \mu\text{m}$  thickness by using sequentially lower beam currents at 30 keV energy (starting at 1 nA and ending at 0.5 or 0.3 nA). The position of the lamellae was chosen to include a maximum of micropearl cross sections. An internal micromanipulator with a tungsten needle was used to lift out the pre-thinned lamellae and to transfer them to a copper grid.

Final thinning of the sample to electron transparency ( $\sim 100$  to  $200 \text{ nm}$ ) was carried out on both sides of the lamellae by using sequentially lower beam currents (300 to 50 pA at 30 keV energy). The lamellae underwent only grazing incidence of the ion beam at this stage of the preparation. This allows minimization of ion beam damage and surface implantation of Ga. The thinning progress was observed with SEM imaging of the lamellae at  $52^\circ$ . Electron beam damage was further suppressed by using low electron currents and limiting electron imaging to a strict minimum.

### 2.6 Transmission electron microscopy (TEM) and EDXS analysis

TEM investigations were conducted with a FEI Tecnai G<sup>2</sup> FEG transmission electron microscope operating at 200 kV. In order to document the structural state of micropearls in their pristine undamaged form, selected-area electron diffraction (SAED) patterns were taken directly at the beginning of the TEM session with a broad beam. Scanning TEM (STEM) images were then acquired using a high-angle annular dark field (HAADF) STEM detector (Fischione) with a camera length of 80 mm. EDXS measurements were performed with an EDXS system, model X-MaxN 80T SDD from Oxford. EDXS spectra and maps were recorded in STEM mode. The semiquantitative calculation of the concentrations (including C) was obtained using the Cliff–Lorimer method using pre-calibrated  $k$  factors and an absorption correction integrated into the Oxford software. The absorption correction is based on the principle of electroneutrality, taking into account the valence states and concentrations of cations and oxygen anions. Oxygen is thereby assumed to possess a stoichiometric concentration.

### 3 Results and interpretation

TEM analyses confirmed that the mineral inclusions observed in the *Tetraselmis* species during this study comply with the definition of micropearls given in Martignier et al. (2017) (intracellular inclusions of hydrated ACC, frequently enriched in alkaline-earth elements (e.g., Sr or Ba) and typically displaying internal concentric zonation linked to elemental ratio variations). These mineral inclusions will therefore be named micropearls hereafter.

#### 3.1 SEM observation of micropearls in *Tetraselmis* species

SEM observations of 12 different species of *Tetraselmis* (culture strains), on the day of their arrival from the supplier, show that 10 of them contained micropearls (Fig. 1, Table 1). None were observed in *T. ascus* and *T. marina*. The general shape of the micropearls in the marine species is elongated, resembling rice grains (Fig. 1 except 1d), while it is spherical in *T. cordiformis* (the only freshwater species of this study) (Fig. 1d). The micropearls' size (0.4–1.2  $\mu\text{m}$  in length) and shape differ among species. Detailed values for each species are given in Table 1.

Micropearls do not seem to be randomly distributed inside the cells, but rather show a definite location in most species (Figs. 1 and S2). Moreover, for a given species, most cells present a similar micropearl arrangement (Fig. S1). Exceptions are cells that were damaged during sample preparation. Filtration or freshwater rinsing, for example, can disrupt the micropearl distribution pattern (Figs. S1e and f and S3).

In some species, the micropearls are mostly aggregated at one side of the cell, with “pointed” tips appearing at the center of the cell and on both sides, resulting in a “trident” shape. This is the case for *T. chui*, *T. suecica* and *T. tetrathele* (Fig. 1a, i, j). *T. striata* shows a similar central micropearl distribution, but the lateral points of the trident are absent (Fig. 1g). In *T. suecica* the central micropearl alignment is generally longer and not necessarily connected to the apical aggregate (Fig. 1i). *T. levis* (Fig. 1f) also shows a similar arrangement, but the aggregate is missing, leaving the micropearls to form three longitudinal alignments (meridians). Altogether, *T. chui*, *T. levis*, *T. suecica* and *T. tetrathele* present patterns with an approximately similar trimerous radial organization (although a tetramerous symmetry cannot be totally excluded as dried samples do not allow a definite judgement). Observations seem to indicate that, in most species, the micropearl aggregate is located at the apical side of the cell (near the apical depression from which the four flagella emerge) (Fig. S2). In *T. convolutae* (Fig. 1c), the micropearls form a small aggregate at the basal extremity of the cell, while larger polyphosphate inclusions gather at the opposite (apical) side.

A different and interesting organization of the micropearls is displayed by both *T. desikacharyi* (Fig. 1e) and *T. con-*

*tracta* (Fig. 1b). An apical aggregate of micropearls is generally present, while other micropearls form regularly spaced meridians, which, in *T. contracta*, extend from the apical pole towards the basal part of the cell (Figs. 1b and S2). These meridians are not well expressed in all cells but, when they are clearly visible, there seems to be around eight or 10 of them inside the cell. When well preserved, the micropearl organization in *T. cordiformis* also shows multiple micropearl alignments that depart from a well-developed apical aggregate, although the alignments are generally well arranged only close to the aggregate and the size of micropearls decreases quickly towards the basal end of the cell (Fig. 1d). Finally, samples observed in this study do not allow us to state if there is a definite distribution of the micropearls in *T. subcordiformis* (Figs. 1h and S2).

Polyphosphate inclusions are frequently observed in *Tetraselmis* species. Their distribution seems to be random except in *T. convolutae* (Fig. 1c). Aggregates of small iron oxide minerals were frequently observed in dried samples at one extremity of *T. desikacharyi* and *T. convolutae* (Fig. 1c and e) – probably at the apical extremity. EDXS analyses performed in both polyphosphate inclusions and iron oxide aggregates are shown in Fig. S4.

In order to compare our results with members of another genus, we also analyzed other flagellate species (e.g., *Chlamydomonas reinhardtii* and *Chlamydomonas intermedia*) obtained from algal culture collections (Table 1). No calcium carbonate inclusions were observed in these cells. Thorough observation of samples from Lake Geneva confirms that not all flagellates produce micropearls. This biomineralization process seems to be exclusive to a limited number of species.

Table 2 shows the result of counts carried out on the species producing micropearls. On average, 77 % of the cells contained micropearls and amongst these, 51 % showed the pattern that is characteristic of their species. This last value is high, considering that all cells do not fall onto the filter with the same orientation and that the only patterns we consider are those obtained when the cell is deposited on its lateral side. Patterns resulting from a deposition of the cells on their apical or basal sides are not considered because the 3-D repartition of the micropearls in the cells is still uncertain.

#### 3.2 TEM observation of FIB-cut cross sections of micropearls

FIB-cut cross sections of micropearls produced by *T. chui* and *T. suecica* are shown in Fig. 2, where they are compared to a similar section in a cell of the freshwater species *T. cordiformis* sampled in a natural environment (Lake Geneva). The choice of *T. chui* and *T. suecica* for FIB processing and TEM observation was based on the size of the micropearls and on their strong concentration in Sr. Both features were considered to favor the observation of compositional zonation, as observed in our previous study (Martignier et al., 2017). A

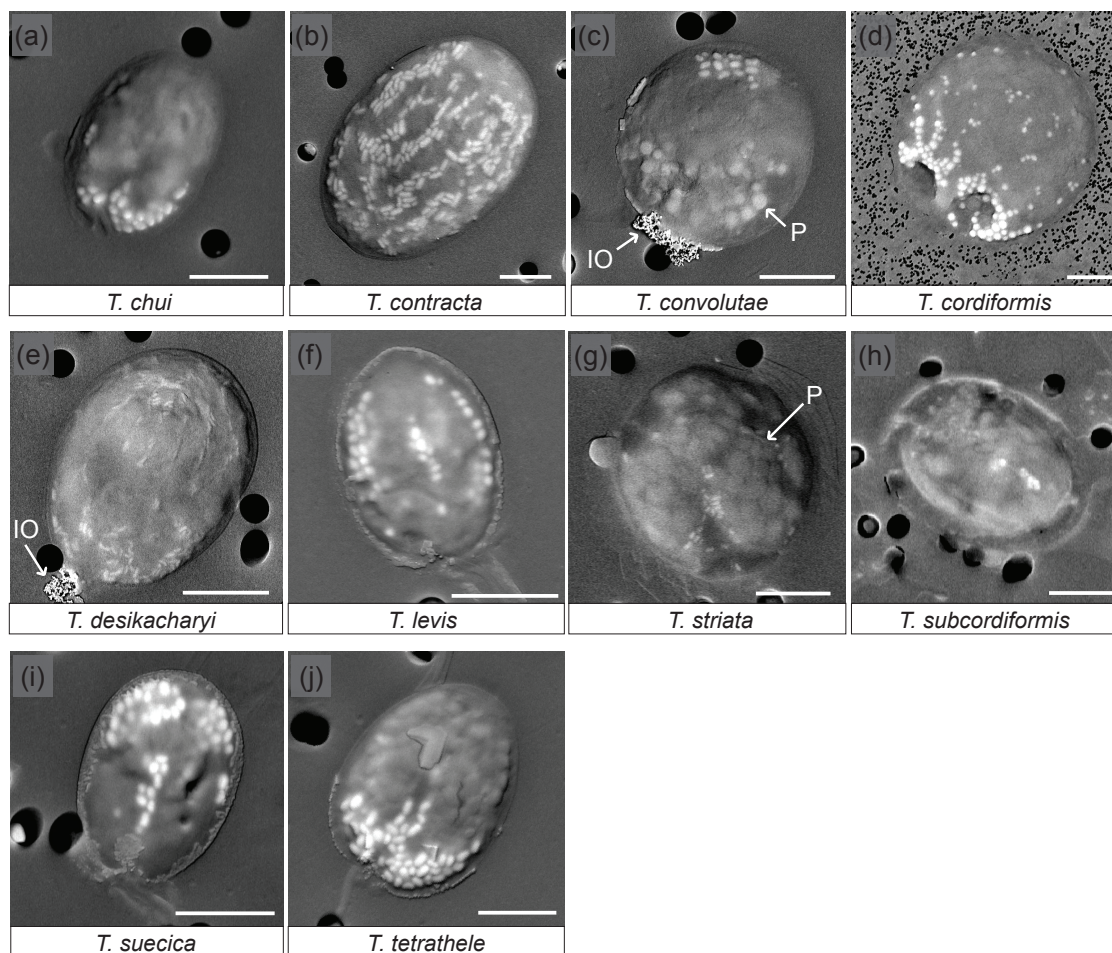


**Figure 1.** SEM images of 10 *Tetraselmis* species containing micropearls at the time of observation. Backscattered electron images of dried samples. The micropearls appear in white or light grey against the darker organic matter, as elongated shapes, except for *T. cordiformis* (d), for which they are spherical. P: the larger and slightly darker inclusions are polyphosphates (c, g). IO: iron oxides. Pores of the filters are visible as black circles in the background (2  $\mu\text{m}$  in diameter except for d: 0.2  $\mu\text{m}$ ). Strains are as follows. (a): chui\_cc; (d): cord\_M\_cc; (j): tetraethe\_ac. Scale bars are 5  $\mu\text{m}$ .

FIB cut was also performed in a *Tetraselmis contracta* cell. This result is shown separately in Fig. 3 because the very good conservation of the organic matter in this sample allows the simultaneous observation of other intracellular constituents.

Micropearls in all four species show strong similarities. They are located inside the organic envelope, are amorphous (Figs. 2 and 3) and, except for the sample with pure Ca (*T. contracta* in Fig. 3), they show a distinct internal concentric zonation (Fig. 2). In all observed species, the cut sections of micropearls suggest the presence of a rod-shaped nucleus in their center (Figs. 2 and S5).

As already pointed out, the micropearls are extremely sensitive to the action of the electron beam (Martignier et al., 2017), indicating a vaporization of some of its components: organic matter associated with water, water contained in the amorphous calcium carbonate (Rodríguez-Blanco et

al., 2008) or both. This ACC seems to be rather stable, as beam sensitivity persists after more than 5 months of storage of dry samples at room temperature.

TEM–EDXS analyses show that the zonation observed in the marine micropearls of *T. chui* and *T. suecica* (Figs. 2 and S6) is due to changes in the Sr/Ca concentration ratios, similar to the zonation observed in the freshwater micropearls in *Tetraselmis* cf. *cordiformis* (Martignier et al., 2017). All micropearls within one cell do not necessarily have an identical composition. An example is shown in Fig. 2a, in which one micropearl possesses a composition with a higher atomic mass than the rest (lighter grey level in STEM–HAADF image) due to a higher content of Sr. Furthermore, micropearls within one cell display variable zonation patterns, as thickness and intensity of the zones differ (Fig. 2a and c).

**Table 2.** Percentage of cells presenting micropearls and specific patterns of micropearl arrangement. Percentage of cells presenting micropearls for each strain and percentage of these cells showing the typical micropearl arrangement pattern for that species (see Figs. 1 and S1). Two strains have been analyzed for *T. chui* and *T. cordiformis*. Please note that strains grown on agar generally show a much lower presence of micropearls and were not considered for the statistics. The asterisk marks a single sample taken 60 days after the strain's arrival in our laboratory, while all the others were observed on the first day after arrival from the provider. This exception allowed us to estimate the number of cells showing the micropearl arrangement pattern of this species, as both samples of *T. cordiformis* strains taken on the first day were damaged during sample preparation by too strong of a filtration. On the first day after arrival, strain CCAC 0579B gave results similar to those of strain CCAC 0051. mp: micropearls. For details on providers and media, see Table 1.

<i>Tetraselmis</i>	Strain	Medium	Total cells counted	% cells with mp/cells	% pattern/cells with mp	Remarks
<i>T. chui</i>	CCAC 0014	ASP-H	160	93	40	
<i>T. chui</i>	SAG 8-6	1/2 SWEg Ag	121	40	37	Resuspended from agar
<i>T. contracta</i>	CCAC 1405	ASP-H	103	98	79	
<i>T. convolutae</i>	CCAC 0100	ASP-H	100	40	70	
<i>T. cordiformis</i>	CCAC 0051	SFM	115	60	0	Strongly filtered
<i>T. cordiformis</i> *	CCAC 0579B	Waris-H	123	98	46	Gently filtered
<i>T. desikacharyi</i>	CCAC 0029	ASP-H	122	25	13	
<i>T. levis</i>	AC 257	ES	123	94	51	
<i>T. striata</i>	SAG 41.85	SWES (agar)	136	12	25	Resuspended from agar
<i>T. subcordiformis</i>	SAG 161-1a	Porph (agar)	100	1	0	Resuspended from agar
<i>T. suecica</i>	AC 254	ES	105	99	57	
<i>T. tetrathele</i>	AC 261	ES	101	89	56	

### 3.3 TEM–EDXS mapping: location of the micropearls inside a *Tetraselmis contracta* cell

The coexistence of micropearls with other cellular constituents and their respective positions in the cell are shown by a TEM image of a FIB-cut section through a *T. contracta* cell (Fig. 3). The micropearls of this species are large and numerous and nearly exclusively consist of ACC without detectable Sr (Fig. S6). They appear as round to ovoid light grey shapes with smooth surfaces (Fig. 3a). TEM observations also reveal that most micropearls are not randomly scattered throughout the cell but are located preferentially just under the cell wall.

Although Fig. 3a is difficult to interpret because of the atypical preparation of the sample (simply dried instead of more traditional preparations for TEM observation such as chemical fixation or cryosections), the identification of the visible cellular constituents can still be attempted (Figs. 3b and S7). Side views (lower part of the section) and tangential sections of starch grains (upper part of the section) are visible, as well as a glancing view of the chloroplast, which is reticulated in this species. Although micropearls resemble starch grains at first look, it is quite easy to differentiate them. First, they are generally more rounded than starch grains, and secondly they are not located inside the chloroplast; in particular, they are not associated with the prominent pyrenoid.

TEM–EDXS mapping provides compositional information improving the identification of the cellular constituents and organelles visible in the section (Figs. 3c and S8). Micropearls are very visible, based on the high concentration of Ca, with small quantities of K (and sometimes Mg, not

shown here). The theca, composed of fused scales, appears as a thin layer between the cell and the filter. Its composition including C, Ca, S and small amounts of K makes it apparent in Fig. 3c (in violet). The theca of these organisms is indeed known to contain 4 % of Ca and 6 % of S (as sulfate) by weight (Becker et al., 1994, 1998).

The two irregular features that are highly enriched in P (in green in Fig. 3c) are identified as being polyphosphate (PolyP) inclusions, flattened during sample preparation. Finally, the dark grey features, in the center of the section, are probably mitochondrial profiles.

### 3.4 SEM–EDXS analysis of micropearl composition

The micropearls of most marine species (Fig. 4a) are composed of ACC, with Ca and Sr as cations. This composition is similar to that measured for micropearls of *T. cordiformis* in Lake Geneva (Martignier et al., 2017). We noted two differences from our previous observations: *T. desikacharyi* forms micropearls containing small amounts of Ba and micropearls of *T. contracta* contain low concentrations of K. However, since growth media had different compositions, these differences need to be taken with care.

Figure 4a compiles the composition of the micropearls for each *Tetraselmis* strain (SEM–EDXS analyses), ranked in increasing order of Sr/Ca median values. Even if low concentrations of K are present in micropearls of *T. contracta*, it was not considered because this element is also present in the surrounding organic matter (Fig. S8), making it impossible to estimate the portion of the measured K that belongs to the micropearls. Magnesium was discarded for the same rea-

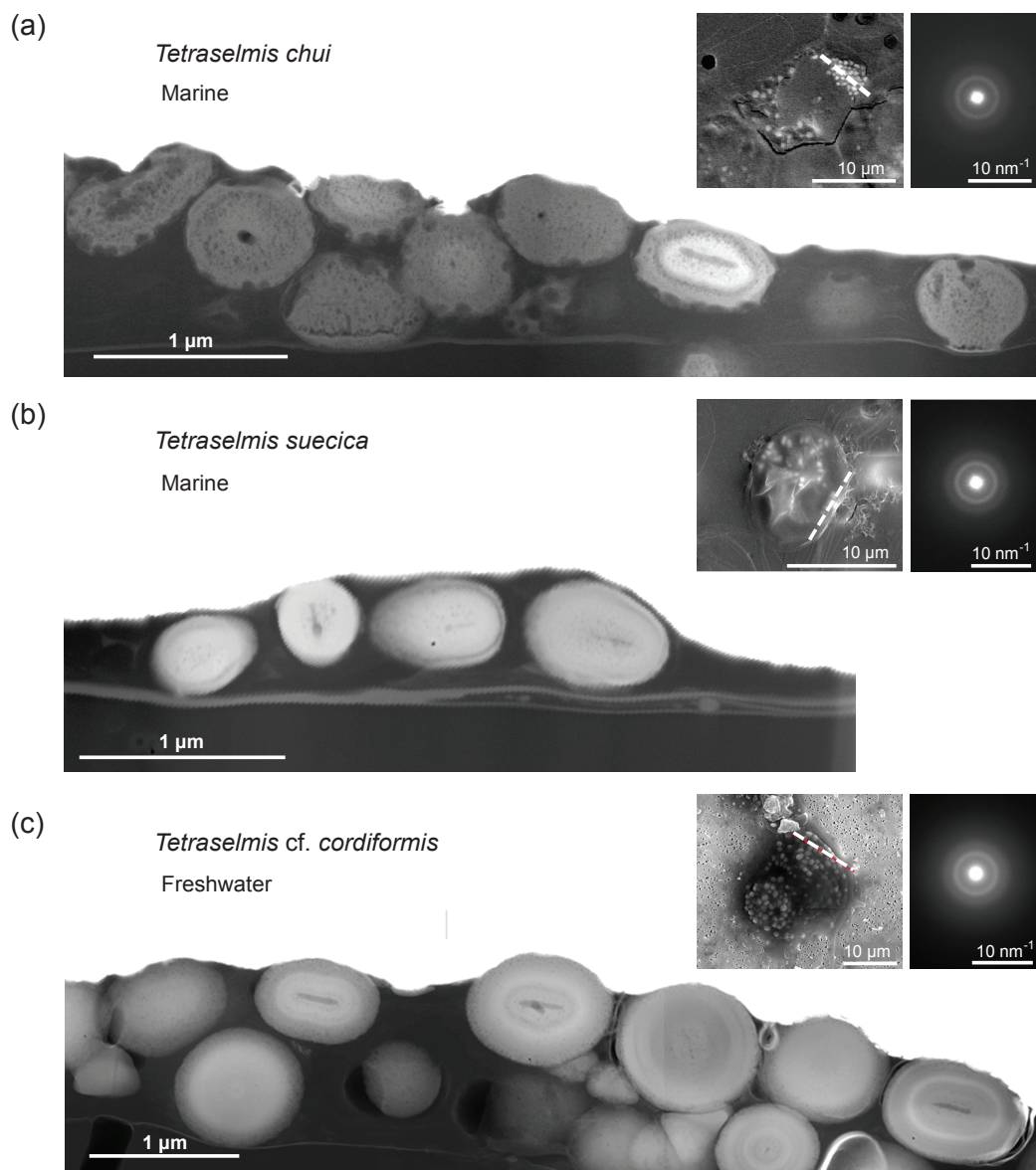


**Figure 2.** Comparison of FIB-cut sections of cells of three different *Tetraselmis* species (dried samples). TEM–HAADF images: FIB-cut sections through cells of (a) *Tetraselmis chui* (culture sample), (b) *Tetraselmis suecica* (culture sample) and (c) *Tetraselmis cf. cordiformis* (Lake Geneva) (Martignier et al., 2017). Small bubbles inside the micropearls (particularly visible in the marine species) are due to beam damage. The contact between the cell and the filter surface is visible near the bottom in each image. Left top insets: SEM secondary images of the whole cell before FIB preparation indicating the location of the cut with a dashed line. Right top insets: SAED patterns from a single micropearl of each FIB-cut section (broad diffraction rings are indicative of amorphous material).

son. It should be noted that the size of micropearls is close to or even below the resolution limit of the SEM–EDXS analysis technique. This means that the interaction volume of the electron beam with the sample is often larger than the micropearls themselves. Therefore the technique yields compositions that include the micropearl and the surrounding organic matter or nearby cellular constituents (e.g., polyphosphates).

### 3.5 ICP-SFMS analysis of Sr/Ca ratio in growth media: data and interpretation

The concentrations of Sr and Ba in the culture media are given in Table S2 and represented graphically in Fig. S9. Strontium concentrations range from  $3.3 \times 10^{-8}$  M (freshwater medium SFM) to  $7.1 \times 10^{-5}$  M (seawater SWES medium). All media have lower Sr concentrations than the average seawater ( $9.1 \times 10^{-5}$  M). SFM, used to grow *T.*

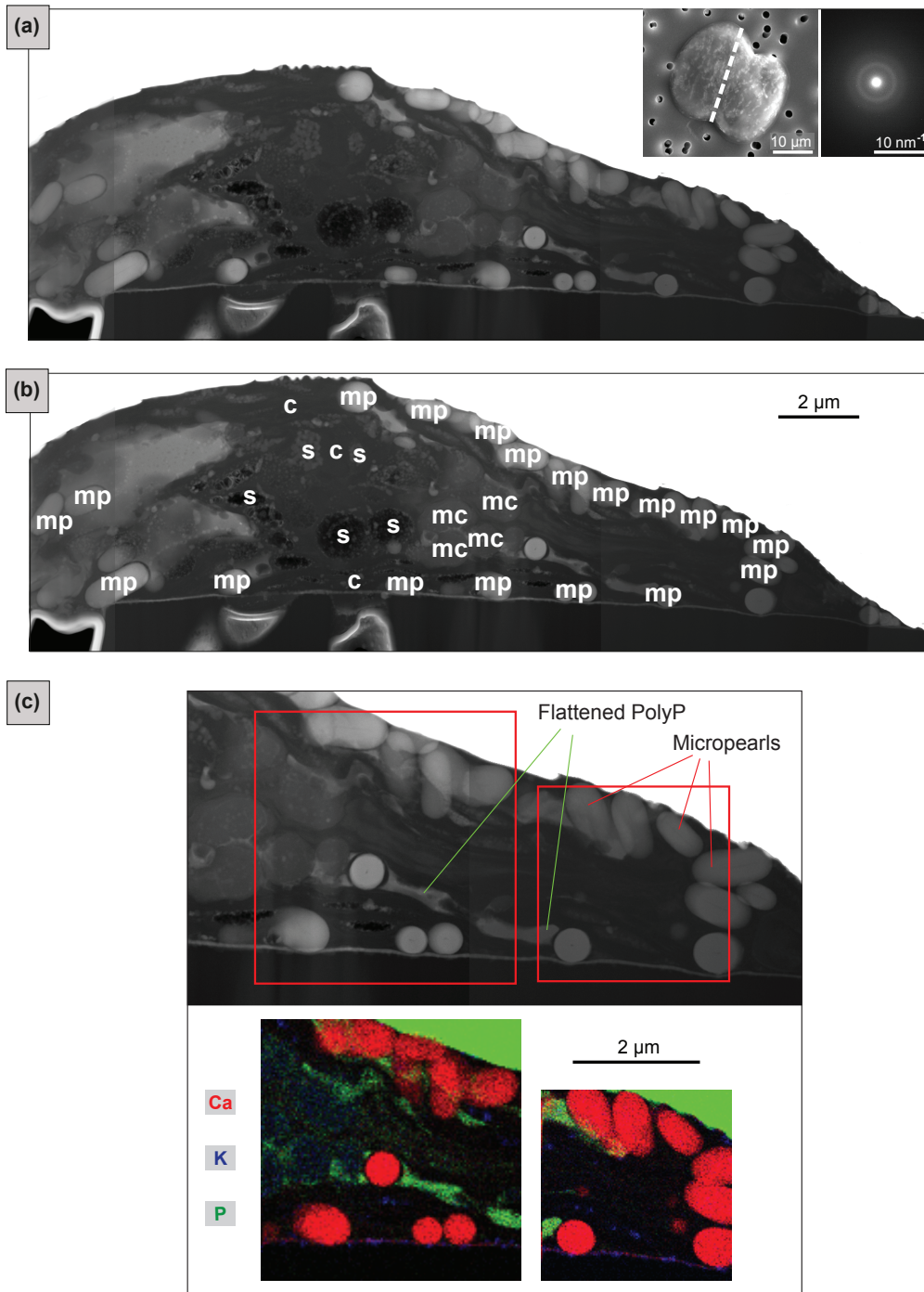


**Figure 3.** FIB-cut section through a *Tetraselmis contracta* cell (dried sample). **(a)** TEM-HAADF image of the whole FIB-cut section. The micropearls show light or medium grey shades and regular round or oval shapes. Left top inset: SEM secondary image of the whole cell before it was cut, with a dashed line indicating the location of the section. Right top inset: SAED patterns from a single micropearl of this FIB-cut section (diffuse diffraction rings are indicative for amorphous material). **(b)** Tentative identification of the visible cellular constituents; s: starch grains; c: chloroplast; mp: micropearls; mc: mitochondria. See Fig. S7 for a detailed image. **(c)** TEM-EDXS mappings – the top image shows the location of the two zones on a TEM-HAADF image of the section. The map shows an RGB image with three superimposed element mappings. Micropearls are mainly composed of Ca, with small quantities of K (and Mg, not shown here). Note that, due to the overlap between the P K peak and secondary Pt L peak, the Pt layer, which was deposited on top of the sample during FIB preparation, is also visible in green.

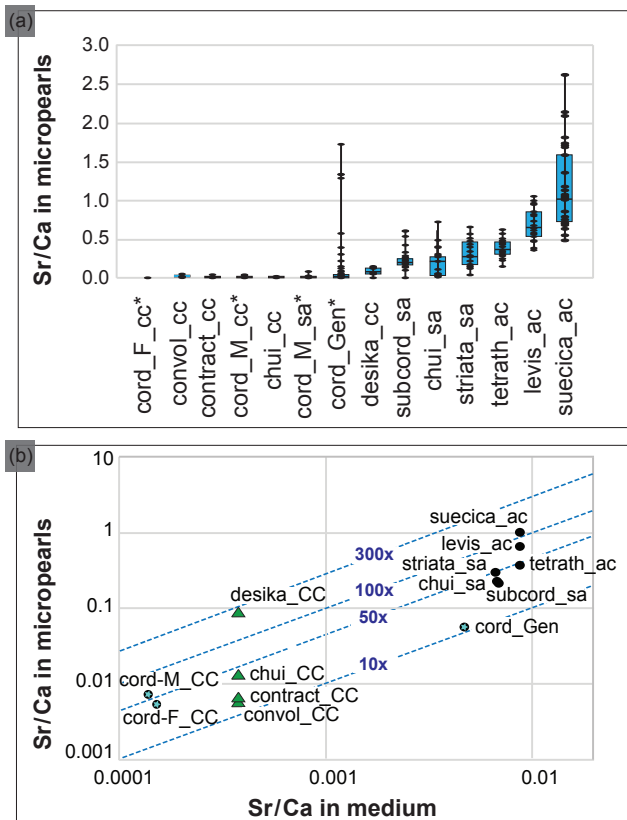


**Figure 4.** Composition of the *Tetraselmis* micropearls and their relation with the growth media composition. **(a)** Distribution of the Sr/Ca ratio for each *Tetraselmis* strain (EDXS analyses), ranked according to the median value of Sr/Ca. At least 20 SEM–EDXS analyses were performed on micropearls of each strain. Asterisks highlight freshwater strains. The range between the minimum and maximum data is shown by black lines. The blue boxes represent the 25–75 % inter-quartiles, while the black horizontal line in the boxes shows the median value. **(b)** Relationship between the composition of the growth media and the composition of the *Tetraselmis* micropearls, expressed as the Sr/Ca ratio. Each point represents the median Sr/Ca ratio measured in each species’ micropearls, related to the Sr/Ca ratio of the growth medium. Points with blue stars highlight freshwater strains. The blue dotted lines define the values of the Sr enrichment factor of the micropearls with respect to the medium (10×, 50×, etc.). Calcium concentrations of the growth media were calculated, based on media theoretical composition. Green triangles signal four samples grown in the same medium. The abbreviations and characteristics of each strain are indicated in Table 1 while Sr/Ca values appear in Table S2 (for medium) and S3 (for micropearls). Results from *T. cordiformis* from Lake Geneva (cord\_Gen) (Martignier et al., 2017) are given as a comparison.

*cordiformis* – the only freshwater strain under study – has lower Sr concentrations than those measured in Lake Geneva ( $5.2 \times 10^{-6}$  M).

The molar ratio Sr/Ca has been calculated for seven growth media (Table S2) and 458 micropearls (Table S3)

in order to evaluate a possible influence of the medium on the micropearls’ composition. Differences among the species regarding the micropearls’ enrichment in Sr compared to their growth medium can be observed. A Sr distribution coefficient (or enrichment factor) was calculated as the molar ratio [(Sr micropearls / Ca micropearls) / (Sr medium / Ca medium)]. Figure 4b shows the relationship between the Sr/Ca ratio measured in the growth media and in the *Tetraselmis* micropearls. For most of the strains, the Sr enrichment factor of the micropearls with respect to the medium varies between 10 and 100 times (see Table S3 for exact figures), with the notable exception of *T. desikacharyi* (more than 200 times). It is interesting to observe that both strains of *T. chui* – from different geographic origins (Table 1) – have rather similar Sr distribution coefficients (around 30), while the three strains of *T. cordiformis* show slightly different enrichment factors (25 for Lake Geneva water, 33 for Lake Fühlingen and 51 for Münster castle moat). Broadly speaking, Sr/Ca increases in micropearls together with its increase in the medium. However, the spread in enrichment may be large for a given medium (such as ASP-H for strains of *T. contracta*, *T. convolutae*, *T. chui* and *T. desikacharyi*).

## 4 Discussion

Micropearls had been previously interpreted as a feature specifically related to freshwater environments (Martignier et al., 2017). The present results show that the biomineralization process leading to the formation of micropearls can take place in very different environments. The following paragraphs aim to discuss our present knowledge on micropearls in general and on their formation process as well as the newly discovered widespread biomineralization capacity in the *Tetraselmis* genus, involving high concentration capacities of these organisms regarding Sr.

### 4.1 Marine and freshwater micropearls

The discovery of micropearls in marine species of *Tetraselmis* shows that this biomineralization process can take place in organisms living in waters of different composition, from freshwater, like Lake Geneva, to seawater (Fig. S9). This highlights the capacity of these organisms to integrate Ca and Sr from different external media.

The production of micropearls is clearly not directly related to a specific habitat since seven *Tetraselmis* species forming micropearls live as phytoplankton in freshwater, marine or brackish waters (Guiry and Guiry, 2018; John et al., 2002); *T. contracta* and *T. desikacharyi* were sampled in the sand, at the bottom of a marine estuary (Marin et al., 1996) or at low tide; and *T. convolutae* is usually observed as a photosymbiont inside a flatworm (Muscatine et al., 1974). Regarding the only two species that did not show micropearls at the

time of observation (*T. ascus* and *T. marina*), it is interesting to note that both live as stalked sessile colonies, with motile life history stages (Norris et al., 1980).

Apart from their elongated shape, marine micropearls have characteristics similar to micropearls formed by the freshwater species *T. cordiformis* (Martignier et al., 2017). Micropearls show a range of possible composition for each species (Fig. 4a and Table S3). The Sr/Ca ratio seems to be influenced by several parameters, amongst which we identified the composition of the culture medium (Fig. 4b) and the Sr concentrating capacity of each *Tetraselmis* species (e.g., green triangles in Fig. 4b). Indeed, the general trend seen in this diagram is an adaptation of the ACC precipitation to the medium composition. However, more relevant information is provided by the enrichment factor (*E* factor; see Table S4 and dotted isolines in Fig. 4b), which allows us to rank species (Table S4) from low values (12–16) to more than 200. This ranking would need to be confirmed by cultivating the species in different media (e.g., *T. convolutae* group in ES and *T. tetrathele* group in ASP-H) and comparing the new enrichment factor with the current values. The very high *E* factor for *T. desikacharyi* can tentatively be linked to distinctive morphological features (a six-layered theca, a novel flagellar hair subtype) not found in other strains of *Tetraselmis* (Marin et al., 1996).

The pattern drawn by the arrangement of the micropearls in the cell is clearly more homogeneous within a strain compared to among strains. Statistics show that these patterns are characteristic for a given species (Table 2 and Fig. S1), which means that the organisms can probably exert a strong control on the number, size and organization of the micropearls in the cells.

#### 4.2 Hints about the formation process of micropearls

The biomineralization process leading to the formation of micropearls seems to start in the same way in all *Tetraselmis* species observed in FIB sections (*T. chui*, *T. contracta*, *T. cordiformis* and *T. suecica*), with a similar rod-shaped nucleus (Figs. 2, 3 and S5). These nuclei could possibly be of an organic nature given their darker appearance in the STEM–HAADF images that point to a material of lower atomic mass (Fig. S5).

It is important to note that there are many parameters which seem to influence the presence and absence of micropearls in the cells: the state of the culture (fully healthy or suffering from the transport, for example), the pH of the medium and probably other parameters we are not yet aware of. For example, the use of agar as a culture medium seems to hinder the development of micropearls (Table 2 and Fig. 1g and h). Nevertheless, the composition of the medium does not seem to influence the arrangement of the micropearls in the cell, as demonstrated by *T. chui*, *T. contracta* and *T. convolutae* (respectively Fig. 1a, c and d), which have different patterns, although all were cultured in the ASP-H medium.

Internal concentric zones are observed in the micropearls formed by cells grown in both the natural environment and cultures (Fig. 2). The presence of this concentric pattern, even when the growth media have a stable composition, may indicate that the zonation is not due to changes in the surrounding water or medium composition during micropearl growth but rather depends on variations in the intracellular fluid composition caused by the biomineralization process itself. In the hypothesis discussed by Thien et al. (2017), it is suggested that the formation of the micropearls results from a combination of a biologically controlled process (preferential intake of specific cations inside the cell) and abiotic physical and chemical mechanisms (mineralization resulting from a nonequilibrium solid-solution growth mechanism, leading to an internal oscillatory zoning). Nevertheless, even that second part of the process does not seem to be purely abiotic, as demonstrated by the long-term amorphous state displayed by micropearls (at least 5 months, according to our observations). Indeed, synthetic ACC with no additives is unstable and rapidly crystallizes into calcite or aragonite (Addadi et al., 2003; Bots et al., 2012; Weiner and Addadi, 2011; Purgstaller, 2016), often through the intermediate form of vaterite (Rodríguez-Blanco et al., 2011). In contrast, long-term stabilization of ACC implies the presence of mineral or organic additives (Aizenberg et al., 2002; Sun et al., 2016). Magnesium is known to play a key role in the stabilization of ACC (Politi et al., 2010). This might well be the case for the *Tetraselmis*-hosted micropearls, in which Mg content is around 2 mol %. Although the phosphate ion has also been reported to inhibit ACC crystallization (Albéric et al., 2018), that does not seem to be the case here since the phosphorus concentration of the micropearls is below the detection level of EDXS. Stabilization of ACC is also enhanced by certain proteins, polyphosphonates, citrates and amino acids (Levi-Kalishman et al., 2002; Addadi et al., 2003; Cam et al., 2015; Cartwright et al., 2012). The presence of these molecules inside the micropearls is suggested by their observed sensitivity to beam damage. As for the possible role of Sr in the ACC long-term stability, we did not find any reference thereof in the literature. However, in an in vitro experiment, Littlewood et al. (2017) found, in the presence of Mg, a correlation between added Sr and the reaction time to transform ACC into calcite (2 h to a maximum of 24 h).

#### 4.3 A new intracellular feature in a well-known genus

Our results (Fig. 1) confirm that artifacts can be induced by the usual biological sample preparation techniques (Martignier et al., 2017) and thus introduce bias in observations and even hide some physiological traits in otherwise well-studied organisms. Figure 3c shows that the straightforward sample preparation method used in this study (dried, with no chemical fixation) allows the preservation of the micropearls and yields useful data on the composition of the different ele-

ments present inside the cell, without any chemical disturbance.

Micropearls represent a new intracellular feature. Their systematic presence in most of the analyzed *Tetraselmis* species suggests that they probably play a physiological role. A possible explanation could be that micropearls increase the sedimentation rate of cells that shed their flagella upon N starvation at the end of *Tetraselmis* blooms. An alternative hypothesis is that micropearls represent reserves of Ca for periods when millimolar Ca is not available in the external medium. Indeed, most Chlorodendrophyceae are known to require the presence of Ca<sup>++</sup> to survive and multiply (Melkonian, 1982). The evolutionary diversification of this class occurs in the marine habitat, where the Ca concentration is constantly around 10 mM (Table 4.1 in Pilson, 1998). The need for Ca is supported by *T. cordiformis*, the only freshwater species of the genus, occurring only in Ca-rich lakes, with a minimum of 1 mM of Ca (e.g., Lake Geneva (1 mM) or Lake Fühlinger (2 mM)), and tests on cultures showed that *T. cordiformis* cannot develop normally in an environment with 0.42 mM of Ca (Melkonian, 1982). Calcium is needed to support phototaxis (light-oriented movements) and for the construction and maintenance of cell coverage (theca, flagellar scales) (Becker et al., 1994; Halldal, 1957). The Sr found in the composition of the micropearls formed by most *Tetraselmis* spp. (Fig. 4) could be transported by the same transporter as Ca. Indeed, Chlorodendrophyceae have very efficient light-gated Ca channels (channelrhodopsins), which are also essential for phototaxis of these flagellates (Govorunova et al., 2013; Halldal, 1957).

#### 4.4 Bioremediation possibilities

The capacity of some organisms to concentrate Sr is of great interest regarding bioremediation. Strontium (<sup>90</sup>Sr) is one of the radioactive nuclides released in large quantities by accidents such as Chernobyl or Fukushima (Casacuberta et al., 2013) and a major contaminant in wastewater and sludge linked with nuclear activities (Bradley et al., 1996). Its relatively long half-life of ~ 30 years and high water solubility cause persistent water pollution (Thorpe et al., 2012; Yablokov et al., 2009). For example, the desmid green alga *Closterium moniliferum*, which can incorporate 45 mol % of Sr in barite crystals, is considered to be a potential candidate as a bioremediation agent (Krejci et al., 2011). The high Sr absorption capacity of several *Tetraselmis* species also led to their mention as potential candidates for radioactive Sr bioremediation (Fukuda et al., 2014; Li et al., 2006). In our experiments, *T. suecica*, for instance, produced a high number of micropearls that contained more than 50 mol % of Sr when cultured in the ES medium (data not shown). Nevertheless, the process allowing these microorganisms to concentrate Sr had not yet been investigated and further studies of micropearl formation processes could therefore lead to new bioremediation techniques. The genus *Tetraselmis* presents the ad-

ditional advantage of including species living in diverse habitats, which might offer interesting bioremediation applications in different aquatic environments including freshwater, brackish lakes, open sea and hypersaline lagoons (Table 1).

## 5 Conclusions

Until recently, nonskeletal intracellular inclusions of calcium carbonate were considered nonexistent in unicellular eukaryotes (Raven and Knoll, 2010). After the first observation of at least two micropearl-forming organisms in Lake Geneva (Martignier et al., 2017), the present study shows that these amorphous calcium carbonate (ACC) inclusions are widespread in a common phytoplankton genus (*Tetraselmis*), not only in freshwater, but also in seawater and brackish environments. This newly discovered biomineralization process therefore takes place in media of very different composition and our results suggest that it is similar in all studied species: an oscillatory zoning process that starts from an organic rod-shaped nucleus. Although frequent in this well-studied genus, these mineral inclusions had been overlooked in the past, possibly destroyed by the usual sample preparation techniques for electron microscopy. Thus other microorganisms could have similar capacities and intracellular inclusions of ACCs may be more widespread than currently known.

Micropearls represent a new intracellular feature. This study shows that they can be clearly distinguished from other cellular constituents and are not randomly distributed in the cell. On the contrary, micropearls seem to be essentially located just under the cell wall and they draw a pattern that seems to be characteristic for each species. Strong correlations hint that this might have a link with the species habitat.

It appears that, for most of the observed *Tetraselmis* species, the biomineralization process leading to the formation of micropearls enables a selective concentration of Sr. The elements concentrated in the micropearls, as well as their degree of enrichment, seem to be characteristic for each species. Selecting the species with the highest concentration capacities could be of high interest for bioremediation, especially regarding radioactive Sr contaminations linked with nuclear activities.

**Data availability.** All data are directly presented in the article and in the Supplement.

**Supplement.** The supplement related to this article is available online at: <https://doi.org/10.5194/bg-15-6591-2018-supplement>.

**Author contributions.** AM designed and led the study, conducted the SEM and EDXS analysis, analyzed EDXS results and SEM images, and wrote the paper. MF was a key collaborator for writing the

article and provided expertise and key contacts. JMJ and MF helped design the study. JMJ carried out most sample preparations and processed EDXS data. KP produced the FIB sections, conducted the TEM analysis and processed the results. MM interpreted the TEM images of the *T. contracta* cross section and provided biological expertise as a specialist of the genus *Tetraselmis*. MB led the ICP-MS analyses of the growth media. FB provided key contacts and biological advice. FL contributed to the FIB-TEM study. DA is AM's thesis supervisor; he helped design the study, provided expertise and funded the project. All authors discussed the results and commented on the paper.

**Competing interests.** The authors declare that they have no conflict of interest.

**Acknowledgements.** This research was supported by the Société Académique de Genève (Requête 2017/66) and the Ernst and Lucie Schmidheiny Foundation. We thank Mauro Tonolla, Sophie de Respinis and Andreas Bruder (SUPSI) as our collaboration triggered the present research, Barbara Melkonian and the CCAC (University of Cologne) for their help and collaboration, and Maike Lorenz (SAG – University of Göttingen) for culture tips and allowing the analysis of their growth medium. We also thank Stephan Jacquet and Andrew Putnis for advice, as well as Rossana Martini and Camille Thomas for support. The critical and constructive comments of the three reviewers are gratefully acknowledged. Falko Langenhorst is grateful to the Deutsche Forschungsgemeinschaft for funding of the FIB-TEM facilities via the Gottfried-Wilhelm Leibniz program (LA830/14-1).

Edited by: Lennart de Nooijer

Reviewed by: Adrian Immenhauser, Estelle Couradeau, and Marie Alberic

## References

- Addadi, L., Raz, S., and Weiner, S.: Taking advantage of disorder: Amorphous calcium carbonate and its roles in biomineralization, *Adv. Mater.*, 15, 959–970, <https://doi.org/10.1002/adma.200300381>, 2003.
- Aizenberg, J., Lambert, G., Weiner, S., and Addadi, L.: Factors involved in the formation of amorphous and crystalline calcium carbonate: a study of an ascidian skeleton, *J. Am. Chem. Soc.*, 124, 32–39, <https://doi.org/10.1021/ja016990l>, 2002.
- Alberic, M., Bertinetti, L., Zou, Z., Fratzi, P., Habraken, W., and Politi, Y.: The crystallization of amorphous calcium carbonate is kinetically governed by ion impurities and water, *Adv. Sci.*, 5, 1701000, <https://doi.org/10.1002/advs.201701000>, 2018.
- Asinari di San Marzano, C.-M., Legros, A., Piron, C., Sironval, C., Nyns, E.-J., and Naveau, H. P.: Methane production by anaerobic digestion of algae, in: *Energy from biomass: Proceedings of the EC Contractors' Meeting held in Copenhagen, 23–24 June 1981*, edited by: Chartier, P. and Palz, W., Springer Netherlands, Dordrecht, 113–120, 1981.
- Azma, M., Mohamed, M. S., Mohamad, R., Rahim, R. A., and Ariff, A. B.: Improvement of medium composition for heterotrophic cultivation of green microalgae, *Tetraselmis suecica*, using response surface methodology, *Biochem. Eng. J.*, 53, 187–195, <https://doi.org/10.1016/j.bej.2010.10.010>, 2011.
- Becker, B., Marin, B., and Melkonian, M.: Structure, composition, and biogenesis of prasinophyte cell coverings, *Protoplasma*, 181, 233–244, <https://doi.org/10.1007/BF01666398>, 1994.
- Becker, B., Melkonian, M., and Kamerling, J. P.: The cell wall (theca) of *Tetraselmis striata* (chlorophyta): macromolecular composition and structural elements of the complex polysaccharides, *J. Phycol.*, 34, 779–787, <https://doi.org/10.1046/j.1529-8817.1998.340779.x>, 1998.
- Benzerara, K., Skouri-Panet, F., Li, J., Férard, C., Gugger, M., Laurent, T., Couradeau, E., Ragon, M., Cosmidis, J., Menguy, N., Margret-Oliver, I., Tavera, R., López-García, P., and Moreira, D.: Intracellular Ca-carbonate biomineralization is widespread in cyanobacteria, *P. Natl. Acad. Sci. USA*, 111, 10933–10938, <https://doi.org/10.1073/pnas.1403510111>, 2014.
- Blondeau, M., Sachse, M., Boulogne, C., Gillet, C., Guigner, J.-M., Skouri-Planet, F., Poinsot, M., Ferard, C., Miot, J., and Benzerara, K.: Amorphous calcium carbonate granules form within an intracellular compartment in calcifying cyanobacteria, *Front. Microbiol.*, 9, 1768, <https://doi.org/10.3389/fmicb.2018.01768>, 2018.
- Bolton, C. T., Hernández-Sánchez, M., Fuertes, M.-A., González-Lemos, S., Abrevaya, L., Mendez-Vicente, A., Flores, J.-A., Probert, I., Giosan, L., Johnson, J., and Stoll, H. M.: Decrease in coccolithophore calcification and CO<sub>2</sub> since the middle Miocene, *Nat. Commun.*, 7, 10284, <https://doi.org/10.1038/ncomms10284>, 2016.
- Bots, P., Benning, L. G., Rodriguez-Blanco, J.-D., Roncal-Herrero, T., and Shaw, S.: Mechanistic insights into the crystallization of amorphous calcium carbonate (ACC), *Cryst. Growth Des.*, 12, 3806–3814, <https://doi.org/10.1021/cg300676b>, 2012.
- Bradley, D. J., Frank, C. W., and Mikerin, Y.: Nuclear contamination from weapons complexes in the former Soviet Union and the United States, *Phys. Today*, 49, 40–45, <https://doi.org/10.1063/1.881495>, 1996.
- Cam, N., Georgelin, T., Jaber, M., Lambert, J. F., and Benzerara, K.: In vitro synthesis of amorphous Mg-, Ca-, Sr- and Ba-carbonates: What do we learn about intracellular calcification by cyanobacteria?, *Geochim. Cosmochim. Ac.*, 161, 36–49, <https://doi.org/10.1016/j.gca.2015.04.003>, 2015.
- Cartwright, J. H. E., Checa, A. G., Gale, J. D., and Sainz-díaz, C. I.: Calcium carbonate polymorphism and its role in biomineralisation?: How many ACCs are there?, *Angew. Chemie Int. Edit.*, 51, 11960–11970, <https://doi.org/10.1002/anie.201203125>, 2012.
- Casacuberta, N., Masqué, P., Garcia-Orellana, J., Garcia-Tenorio, R., and Buesseler, K. O.: <sup>90</sup>Sr and <sup>89</sup>Sr in seawater off Japan as a consequence of the Fukushima Dai-ichi nuclear accident, *Biogeosciences*, 10, 3649–3659, <https://doi.org/10.5194/bg-10-3649-2013>, 2013.
- Couradeau, E., Benzerara, K., Gérard, E., Moreira, D., Bernard, S., Brown Jr., G. E., and López-García, P.: An early-branching microbialite cyanobacterium forms intracellular carbonates, *Science*, 336, 459–462, <https://doi.org/10.1126/science.1216171>, 2012.
- Domozych, D. S.: The crystalline cell wall of *Tetraselmis convolutae* (Chlorophyta): a freeze fracture analysis, *J. Phycol.*, 20, 415–418, <https://doi.org/10.1111/j.0022-3646.1984.00415.x>, 1984.

- Douglas, A. E.: Uric acid utilization in *Platymonas convolutae* and symbiotic *Convolvata roscoffensis*, *J. Mar. Biol. Assoc. UK*, 63, 435–447, <https://doi.org/10.1017/S0025315400070788>, 1983.
- Dupraz, C., Reid, R. P., Braissant, O., Decho A. W., Norman, R. S., and Visscher, P. T.: Processes of carbonate precipitation in modern microbial mats, *Earth-Sci. Rev.*, 96, 141–162, <https://doi.org/10.1016/j.earscirev.2008.10.005>, 2009.
- Fukuda, S., Iwamoto, K., Atsumi, M., Yokoyama, A., Nakayama, T., Ishida, K., Inouye, I., and Shiraiwa, Y.: Global searches for microalgae and aquatic plants that can eliminate radioactive cesium, iodine and strontium from the radio-polluted aquatic environment: A bioremediation strategy, *J. Plant Res.*, 127, 79–89, <https://doi.org/10.1007/s10265-013-0596-9>, 2014.
- Gooday, G. W.: A physiological comparison of the symbiotic alga *Platymonas convolutae* and its free-living relatives, *J. Mar. Biol. Assoc. UK*, 50, 199–208, <https://doi.org/10.1017/S0025315400000710>, 1970.
- Govorunova, E. G., Sineshchekov, O. A., Li, H., Janz, R., and Spudich, J. L.: Characterization of a highly efficient blue-shifted channelrhodopsin from the marine alga *Platymonas subcordiformis*, *J. Biol. Chem.*, 288, 29911–29922, <https://doi.org/10.1074/jbc.M113.505495>, 2013.
- Grierson, S., Strezov, V., Bray, S., Mummacari, R., Danh, L. T., and Foster, N.: Assessment of bio-oil extraction from *Tetraselmis chui* microalgae comparing supercritical CO<sub>2</sub>, solvent extraction, and thermal processing, *Energ. Fuel.*, 26, 248–255, <https://doi.org/10.1021/ef2011222>, 2012.
- Guiry, M. D. and Guiry, G. M.: *AlgaeBase*, World-wide Electron. Publ. Natl. Univ. Ireland, Galw., available at: <http://www.algaebase.org>, last access: 30 June 2018.
- Halldal, P.: Importance of calcium and magnesium ions in phototaxis of motile green algae, *Nature*, 179, 215–216, <https://doi.org/10.1038/179215b0>, 1957.
- Hemaiswarya, S., Raja, R., Ravi Kumar, R., Ganesan, V., and Anbazhagan, C.: Microalgae: A sustainable feed source for aquaculture, *World J. Microb. Biot.*, 27, 1737–1746, <https://doi.org/10.1007/s11274-010-0632-z>, 2011.
- Jaquet, J. M., Nirel, P., and Martignier, A.: Preliminary investigations on picoplankton-related precipitation of alkaline-earth metal carbonates in meso-oligotrophic lake Geneva (Switzerland), *J. Limnol.*, 72, 592–605, <https://doi.org/10.4081/jlimnol.2013.e50>, 2013.
- John, D. M., Whitton, B. A., and Brook, A. J.: *The freshwater algal flora of the British Isles: An identification guide to freshwater and terrestrial algae*, Natural History Museum (London) and British Phycological Society, Cambridge University Press, 2002.
- Kirst, G. O.: Ion composition of unicellular marine and freshwater algae, with special reference to *Platymonas subcordiformis* cultivated in media with different osmotic strengths, *Oecologia*, 28, 177–189, <https://doi.org/10.1007/BF00345253>, 1977.
- Krejci, M. R., Finney, L., Vogt, S., and Joester, D.: Selective sequestration of strontium in *Desmid* green algae by biogenic co-precipitation with barite, *ChemSusChem*, 4, 470–473, <https://doi.org/10.1002/cssc.201000448>, 2011.
- Levi-Kalishman, Y., Raz, S., Weiner, S., Addadi, L., and Sagi, I.: Structural differences between biogenic amorphous calcium carbonate phases using X-ray absorption spectroscopy, *Adv. Funct. Mater.*, 12, 43–48, [https://doi.org/10.1002/1616-3028\(20021011\)12:1<43::AID-ADFM43>3.0.CO;2-C](https://doi.org/10.1002/1616-3028(20021011)12:1<43::AID-ADFM43>3.0.CO;2-C), 2002.
- Li, M., Xie, X., Xue, R., and Liu, Z.: Effects of strontium-induced stress on marine microalgae *Platymonas subcordiformis* (Chlorophyta: Volvocales), *Chin. J. Oceanol. Limn.*, 24, 154–160, <https://doi.org/10.1007/BF02842815>, 2006.
- Lim, D. K. Y., Garg, S., Timmins, M., Zhang, E. S. B., Thomas-Hall, S. R., Schuhmann, H., Li, Y., and Schenk, P. M.: Isolation and evaluation of oil-producing microalgae from subtropical coastal and brackish waters, *PLoS One*, 7, e40751, <https://doi.org/10.1371/journal.pone.0040751>, 2012.
- Littlewood, J. L., Shaw, S., and Peacock, C. L.: Mechanism of enhanced strontium uptake into calcite via an amorphous calcium carbonate (ACC) crystallisation pathway, *Cryst. Growth Des.*, 17, 1214–1223, <https://doi.org/10.1021/acs.cgd.6b01599>, 2017.
- Lu, L., Wang, J., Yang, G., Zhu, B., and Pan, K.: Biomass and nutrient productivities of *Tetraselmis chui* under mixotrophic culture conditions with various C:N ratios, *Chin. J. Oceanol. Limn.*, 35, 303–312, <https://doi.org/10.1007/s00343-016-5299-3>, 2017.
- Manton, I. and Parke, M.: Observations on the structure of two species of *Platymonas* with special reference to flagellar scales and the mode of origin of the theca, *J. Mar. Biol. Assoc. UK*, 45, 743–754, <https://doi.org/10.1017/S0025315400016568>, 1965.
- Marin, B., Matzke, C., and Melkonian, M.: Flagellar hairs of *Tetraselmis* (Prasinophyceae): Ultrastructural types and intrageneric variation, *Phycologia*, 32, 213–222, <https://doi.org/10.2216/i0031-8884-32-3-213.1>, 1993.
- Marin, B., Hoef-Emden, K., and Melkonian, M.: Light and electron microscope observations on *Tetraselmis desikacharyi* sp. nov. (Chlorodendrales, Chlorophyta), *Nova Hedwigia*, 112, 461–475, 1996.
- Martignier, A., Pacton, M., Filella, M., Jaquet, J.-M., Barja, F., Pollok, K., Langenhorst, F., Lavigne, S., Guagliardo, P., Kilburn, M. R., Thomas, C., Martini, R., and Ariztegui, D.: Intracellular amorphous carbonates uncover a new biomineralization process in eukaryotes, *Geobiology*, 15, 240–253, <https://doi.org/10.1111/gbi.12213>, 2017.
- Mass, T., Giuffrè, A. J., Sun, C.-Y., Stiffler, C. A., Frazier, M. J., Neder, M., Tamura, N., Stan, C. V., Marcus, M. A., and Gilbert, P. U. P. A.: Amorphous calcium carbonate particles form coral skeletons, *P. Natl. Acad. Sci. USA*, 114, E7670–E7678, <https://doi.org/10.1073/pnas.1707890114>, 2017.
- Melkonian, M.: An ultrastructural study of the flagellate *Tetraselmis cordiformis* Stein (Chlorophyceae) with emphasis on the flagellar apparatus, *Protoplasma*, 98, 139–151, <https://doi.org/10.1007/BF01676667>, 1979.
- Melkonian, M.: Effect of divalent cations on flagellar scales in the green flagellate *Tetraselmis cordiformis*, *Protoplasma*, 111, 221–233, <https://doi.org/10.1007/BF01281970>, 1982.
- Montero, M. F., Aristizábal, M., and García Reina, G.: Isolation of high-lipid content strains of the marine microalga *Tetraselmis suecica* for biodiesel production by flow cytometry and single-cell sorting, *J. Appl. Phycol.*, 23, 1053–1057, <https://doi.org/10.1007/s10811-010-9623-6>, 2011.
- Muscatine, L., Boyle, J. E., and Smith, D. C.: Symbiosis of the acoel flatworm *Convolvata roscoffensis* with the alga *Platymonas convolutae*, *P. R. Soc. B*, 187, 221–234, <https://doi.org/10.1098/rspb.1974.0071>, 1974.
- Norris, R. E., Hori, T., and Chihara, M.: Revision of the genus *Tetraselmis* (Class Prasinophyceae), *Bot. Mag. Tokyo*, 93, 317–339, <https://doi.org/10.1007/BF02488737>, 1980.

- Park, J. E. and Hur, S.-B.: Optimum culture condition of four species of microalgae as live food from China, *J. Aquac.*, 13, 107–117, 2000.
- Parke, M. and Manton, I.: The specific identity of the algal symbiont in *Convoluta roscoffensis*, *J. Mar. Biol. Assoc. UK*, 47, 445–464, <https://doi.org/10.1017/S002531540005654X>, 1967.
- Pilson, M. E. Q.: An introduction to the chemistry of the sea, 2nd Edn., Cambridge University Press, 1998.
- Politi, Y., Batchelor, D. R., Zaslansky, P., Chmelka, B. F., Weaver, J. C., Sagi, I., Weiner, S., and Addadi, L.: Role of magnesium ion in the stabilization of biogenic amorphous calcium carbonate: a structure-function investigation, *Chem. Mater.*, 22, 161–166, <https://doi.org/10.1021/cm902674h>, 2010.
- Purgstaller, B., Mavromatis, V., Immenhauser, A., and Dietzel, M.: Transformation of Mg-bearing amorphous calcium carbonate to Mg-calcite – In situ monitoring, *Geochim. Cosmochim. Ac.*, 174, 180–195, <https://doi.org/10.1016/j.gca.2015.10.030>, 2016.
- Raven, J. A. and Knoll, A. H.: Non-skeletal biomineralization by eukaryotes: Matters of moment and gravity, *Geomicrobiol. J.*, 27, 572–584, <https://doi.org/10.1080/01490451003702990>, 2010.
- Regan, D. L.: Other micro-algae, in: *Micro-Algal Biotechnology*, edited by: Borowitzka, M. A. and Borowitzka, L. J., Cambridge University Press, 135–150, 1988.
- Rodriguez-Blanco, J. D., Shaw, S., and Benning, L. G.: How to make “stable” ACC: protocol and preliminary structural characterization, *Mineral. Mag.*, 72, 283–286, <https://doi.org/10.1180/minmag.2008.072.1.283>, 2008.
- Rodriguez-Blanco, J. D., Shaw, S., and Benning, L. G.: The kinetics and mechanisms of amorphous calcium carbonate (ACC) crystallization to calcite, *via* vaterite, *Nanoscale*, 3, 265–271, <https://doi.org/10.1039/C0NR00589D>, 2011.
- Rodriguez-Blanco, J. D., Sand, K. K., and Benning, L. G.: ACC and vaterite as intermediates in the solution-based crystallization of CaCO<sub>3</sub>, in: “New Perspectives on Mineral Nucleation and Growth”, edited by: Van Driessche, A. E. S., Kellermeier, M., Benning, L. G., and Gebauer, D., Springer, 93–111, [https://doi.org/10.1007/978-3-319-45669-0\\_5](https://doi.org/10.1007/978-3-319-45669-0_5), 2017.
- Salisbury, J. L., Baron, A., Surek, B., and Melkonian, M.: Striated flagellar roots: isolation and partial characterization of a calcium-modulated contractile organelle, *J. Cell Biol.*, 99, 962–970, <https://doi.org/10.1083/jcb.99.3.962>, 1984.
- Stein, F. R.: *Der Organismus der Infusionstiere*, III, 1. Hälfte Flagellaten, Engelmann, Leipzig, 1878.
- Sun, S., Chevrier, D. M., Zhang, P., Gebauer, D., and Cölfen, H.: Distinct short-range order is inherent to small amorphous calcium carbonate clusters (< 2 nm), *Angew. Chem. Int. Edit.*, 55, 12206–12209, <https://doi.org/10.1002/anie.201604179>, 2016.
- Thien, B., Martignier, A., Jaquet, J.-M., and Filella, M.: Linking environmental observations and solid solution thermodynamic modeling: The case of Ba- and Sr-rich micropearls in Lake Geneva, *Pure Appl. Chem.*, 89, 645–652, <https://doi.org/10.1515/pac-2017-0205>, 2017.
- Thorpe, C. L., Lloyd, J. R., Law, G. T. W., Burke, I. T., Shaw, S., Bryan, N. D., and Morris, K.: Strontium sorption and precipitation behaviour during bioreduction in nitrate impacted sediments, *Chem. Geol.*, 306–307, 114–122, <https://doi.org/10.1016/j.chemgeo.2012.03.001>, 2012.
- Trench, R. K.: The cell biology of plant-animal symbiosis, *Ann. Rev. Plant Physiol.*, 30, 485–531, <https://doi.org/10.1146/annurev.pp.30.060179.002413>, 1979.
- Venn, A. A., Loram, J. E., and Douglas, A. E.: Photosynthetic symbioses in animals, *J. Exp. Bot.*, 59, 1069–1080, <https://doi.org/10.1093/jxb/erm328>, 2008.
- Wei, L., Huang, X., and Huang, Z.: Temperature effects on lipid properties of microalgae *Tetraselmis subcordiformis* and *Nannochloropsis oculata* as biofuel resources, *Chin. J. Oceanol. Limn.*, 33, 99–106, <https://doi.org/10.1007/s00343-015-3346-0>, 2015.
- Weiner, S. and Addadi, L.: Crystallization pathways in biomineralization, *Ann. Rev. Mater. Res.*, 41, 21–40, <https://doi.org/10.1146/annurev-matsci-062910-095803>, 2011.
- Yablokov, A. V., Nesterenko, V. B., Nesterenko, A. V., and Sherman, J. D.: Chernobyl?: Consequences of the catastrophe for people and the environment, edited by: Sherman-Nevinger, J. D., *Annals of the New York Academy of Sciences*, 327 + 39 pp., 2009.
- Zittelli, G. C., Rodolfi, L., Biondi, N., and Tredici, M. R.: Productivity and photosynthetic efficiency of outdoor cultures of *Tetraselmis suecica* in annular columns, *J. Aquac.*, 261, 932–943, <https://doi.org/10.1016/j.aquaculture.2006.08.011>, 2006.